Anisotropic electrical conduction of vertically-aligned single-walled carbon nanotube films

Cheng-Te Lin [a], Chi-Young Lee [a,b], Tsung-Shune Chin [c], Kei Ishikawa [d], Rong Xiang [d], Junichiro Shiomi [d], and Shigeo Maruyama [d,*]

a Department of Materials Science and Engineering, National Tsing Hua University, Hsinchu, 30013, Taiwan.

b Center of Nanotechnology, Materials Science, and Microsystems, National Tsing Hua University, Hsinchu, 30013, Taiwan.

c Department of Materials Science and Engineering, Feng-Chia University, Taichung, 40724, Taiwan.

d Department of Mechanical Engineering, The University of Tokyo, 7-3-1 Hongo, Bunkyo-ku, Tokyo 113-8656, Japan.

Abstract

Anisotropic electrical conduction measurements have been carried out for thin films of vertically-aligned single-walled carbon nanotubes (VA-SWCNTs) grown by an alcohol catalytic CVD process. Combined with controlled synthesis and structure characterization by optical spectroscopy, the influence of the aligned structure on the electrical conduction has been identified. The out-of-plane conductivity of the films was measured to be about 1.11 S/mm, independently of the film thickness. On the other hand, the in-plane conductivity was found to be more than an order of magnitude smaller, which gives rise to highly anisotropic electrical conduction, reflecting the high degree of alignment in the VA-SWCNT films. The in-plane conductivity decreases with

* Corresponding author. Tel: +81 3 58416421; Fax: +81 3 58006983.

E-mail address: maruyama@photon.t.u-tokyo.ac.jp (S. Maruyama)

increasing film thickness, in contrast to the film of random SWCNT networks, which exhibit thickness-independent in-plane resistance. The thickness-dependent in-plane conductivity can be expounded by a growth model of vertically aligned SWCNT films in which a thin layer of nanotube networks form on top of films at the initial stage of the growth. Such electrical anisotropy of VA-SWCNT films can be useful in miniaturized sensing devices.

1. Introduction

Thin films composed of aligned or random networks of carbon nanotube (CNT) is a promising building block for applications in miniaturized devices, such as energy storage [1], field emitters [2,3], mechanical sensor [4], and molecular sensors [5-9]. The CNT films provide extreme sensitivity and high-density binding sites for sensing molecules of electron-donor (NH_3 [5], N_2 [6] etc.) and electron-acceptor (NO_2 [5], O_2 [7], and SO_2 [8] etc.). CNT-based sensors exhibit a faster response at room temperature and outstandingly higher sensitivity (more than a thousand times) than those of current solid-state sensors, which need to be operated at 300 – 500 ^oC to enhance their chemical reactivity [5,10]. Recently, vertically-aligned single-walled carbon nanotube (VA-SWCNT) films have been successfully fabricated by alcohol CVD process [11,12]. The morphology of vertical alignment indicates that a sensing device can be constructed by directly connecting the as-synthesized films to the electrodes without further treatment. It also avoids the screening effect which usually results in the decrease of originally-high surface area. Combined with a spontaneous detachment technique, the as-prepared VA-SWCNT films can be transferred onto arbitrary

substrates retaining their alignment morphology [13]. This affords a shortcut to flexible conductive VA-SWCNT components, and opens up an opportunity for highly functional chemical sensors.

For the above applications, knowledge in electrical conductivity of VA-SWCNT films is essential. Electrical conductivity of individual multi-walled carbon nanotubes [14,15], aligned SWCNT ropes [16,17] and films [18-20] has been investigated. The reported values fall in the range 6 – 128 S/mm depending on the chirality and extent of intrinsic defects. The conduction mechanism along nanotube axis can be simply explained in terms of the diffusion of valence electrons through overlapping π-electron cloud. On the other hand, in the assembled material, there also exists contact or tunneling junctions between nanotubes [18,21]. Then the electron transport across nanotubes is dominated by the concentration of these contacts or tunneling junctions, resulting in an anisotropic conduction of the aligned nanotube film.

In this study, we have systematically investigated electrical conductivities of VA-SWCNT films along both the out-of- and in-plane directions with a precisely controlled morphology. Although the anisotropic conductivity of aligned multi-walled carbon nanotube material has been examined by several groups [18,22,23], there are limited number of reports available on the conductivity of a SWCNT arrays [19]. Utilizing the technique to synthesize smaller diameter SWCNTs with high alignment and low density, the current work demonstrates a highly anisotropic features of the VA-SWCNT thin film and it sensitivity to the alignment. These understanding plus the technique to deposit electrode patterns on a fragile VA-SWCNT film with a good reproducibility

and feasibility are useful to integrate this anisotropic material into nanoelectronic devices, e.g., conductance-based sensors.

2. Experimental

Using alcohol as the precursor and bimetallic Co-Mo nanoparticles as catalysts, large-area and uniform SWCNT films were prepared on quartz substrate by the alcohol catalytic chemical vapor deposition method [11]. The catalysts were dip-coated in turn using molybdenum and cobalt acetate solutions (dissolved in alcohol) on both sides of the optically polished quartz substrate. For reduction of the acetate to metallic clusters, the dip-coated substrate was baked in air at 400 ^{o}C for 5 min. The reduced metals were then oxidized in air forming monodisperse nanoparticles with 1 – 2 nm in diameter.

For growth of SWCNT films, a piece of substrate coated with Co-Mo catalysts was set in a tube furnace, which had been preheated to 800 ^{o}C with Ar/H_2 (3 %) flow. Then the system was kept at 800 ^{o}C for extra 10 min to reduce the oxide catalysts. Subsequently, vaporized alcohol was injected into the system and the growth process immediately started. The system pressure was maintained at ~ 10 Torr. The thickness of SWCNT film during the growth was *in situ* monitored by measuring the optical absorbance [12]. The *in situ* measurement enables the control of final SWCNT film thickness by terminating promptly the source feeding (termination method). Alternatively, we adopted a method in which the film thickness spontaneously reached an ultimate value after reaction for a longer time (saturation method). The thickness of the film grown by the

saturation method cannot be controlled, thus the samples with appropriate thickness were selected for comparison with that synthesized by the termination method. After the reaction, the heater was turned off and the system was cooled down to room temperature with flowing Ar/H_2. The obtained SWCNT films were characterized by micro-Raman measurements (Seki Technotron: 488 nm) and UV-vis-NIR spectrophotometer (Shimadzu UV-3150).

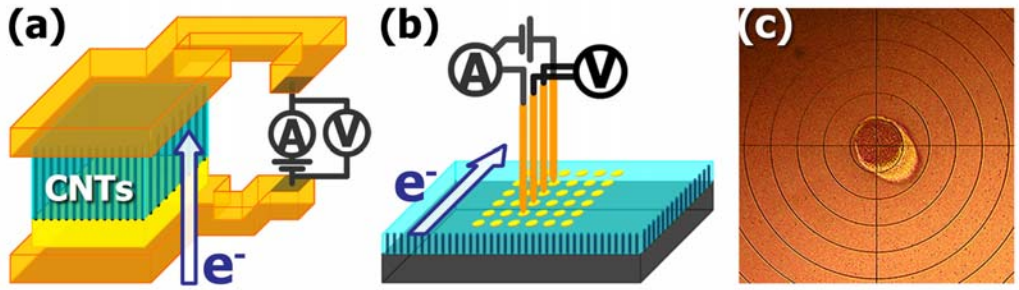

Fig. 1 − The schematics of the devices for studying the electrical properties along (a) out-of-plane and (b) in-plane directions of VA-SWCNT films. (c) The photomicrograph of Ti patterns deposited on the surface of VA-SWCNT films.

For out-of-plane electrical measurements, the SWCNT film was peeled off from the substrate by submersing it into hot water (70 ^{o}C). The freestanding film was then re-attached onto a supporting copper foil used as a bottom electrode with 4 mm^2 in area. Such a transfer procedure has been corroborated not to alter the alignment of SWCNT films [13]. Two copper electrodes were employed to clip this bi-layer sheet, and connected to a semiconductor parameter analyzer (Agilent 4156C) to study the electrical properties in out-of-plane direction of samples (see Fig. 1a). A pressure was applied and gradually increased on the electrodes until the obtained *I-V* plot starts to

correspond to Ohmic contact.

For in-plane electrical measurements, a titanium pattern with 6 × 6 dot-arrays was deposited onto the surface of SWCNT films by thermal evaporation. Each dot pattern was 100 μm in diameter, 500 nm in thickness, and 1 mm in spacing. Four tungsten-needle probes were used to contact the patterns in sequence for in-plane resistance measurements. The device and the photomicrograph of Ti patterns are shown in Fig. 1b and 1c, respectively. Again, a steady pressure was applied between probe and pattern until the obtained *I*-*V* plot is reliable.

3. Results and Discussion

After synthesis, the transparent quartz substrate becomes translucent or opaque black in appearance. The cross-sectional SEM micrograph indicates that a thin layer of aligned SWCNT forest covers the surface of the quartz substrate, as shown in the inset of Fig. 2a. In this figure, the thickness of SWCNT forest is uniform and evaluated to be ~ 5 μm, which can be controlled at will by the termination method utilizing the *in situ* optical absorbance measurement. The absorbance plots of the film thickness versus growth time are shown in Fig. 2a, which demonstrates a successful termination of the growth by stopping the source feeding. Here, the samples with the thicknesses of 0.9, 2.0, 4.2, and 8.3 μm were studied. For comparison, we also prepared a random SWCNT network (0.8 μm), in which the growth density is much lower. Therefore, the SWCNTs tend to extend horizontally. Another sample (8.2 μm) was made by the saturation method, to

examine the effect of synthesis conditions on the electrical properties (see Fig. 2b).

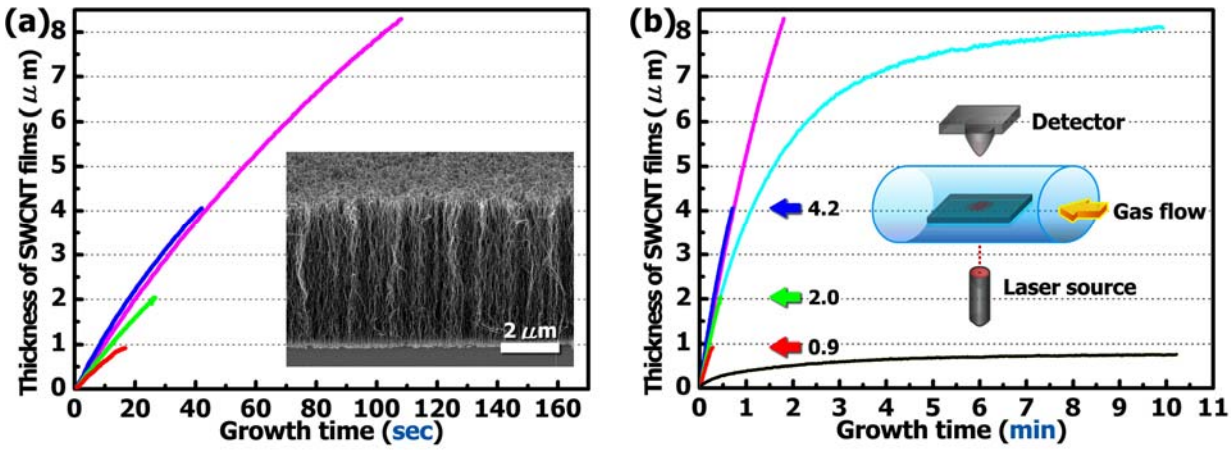

Fig. 2 − The *in situ* absorbance measurements of film thickness versus growth time. The samples were prepared by (a) termination and (b) saturation methods, respectively. (a) The inset shows cross-sectional SEM of a SWCNT forest; (b) Randomly-networked (black line) and 8.2 µm-thick (cyan line) samples were grown until they had approached the growth limit. The thickness measuring optical system is illustrated in the inset.

As shown in Fig. 3a, resonance Raman scattering spectra of all the samples measured using 488 nm laser exhibit the typical features of high-quality SWCNTs; distinct radial breathing modes (RBMs) (100 – 350 cm^{-1}), a small D-band (about 1350 cm^{-1}), and a sharp G-band (1550 – 1605 cm^{-1}). The inset shows enlarged peaks in RBMs. It is noticed that the dominant RBM peak at 180 cm^{-1} is absent for 0.8-µm-thick SWCNT film. The peak has been known as the fingerprint of the vertical alignment of SWCNT films [24], and thus the current result manifests the absence of alignment for 0.8-µm-thick sample. Furthermore, the degree of alignment of the VA-SWCNT films can be identified by p-polarized absorption spectra [25].

Absorption spectra in Fig. 3b for all samples with incident angles (θ) of 0^{o} exhibit the characteristic peaks at ~ 4.5 and/or 5.25 eV. The spectra of the thickest films are out of frame in the high energy range since the transmitted signals were below the detector limit. The peak positions and intensity is closely related to the degree of alignment, where the peak at ~ 4.5 eV is predominant in randomly-oriented SWCNT films while that at ~ 5.25 eV is predominant in vertically-aligned SWCNT films [25]. With this, one can note that the randomly-networked sample (0.8 μm) exhibits no peak at ~ 5.25 eV, in contract to the 0.9-μm-thick film though their thickness is similar.

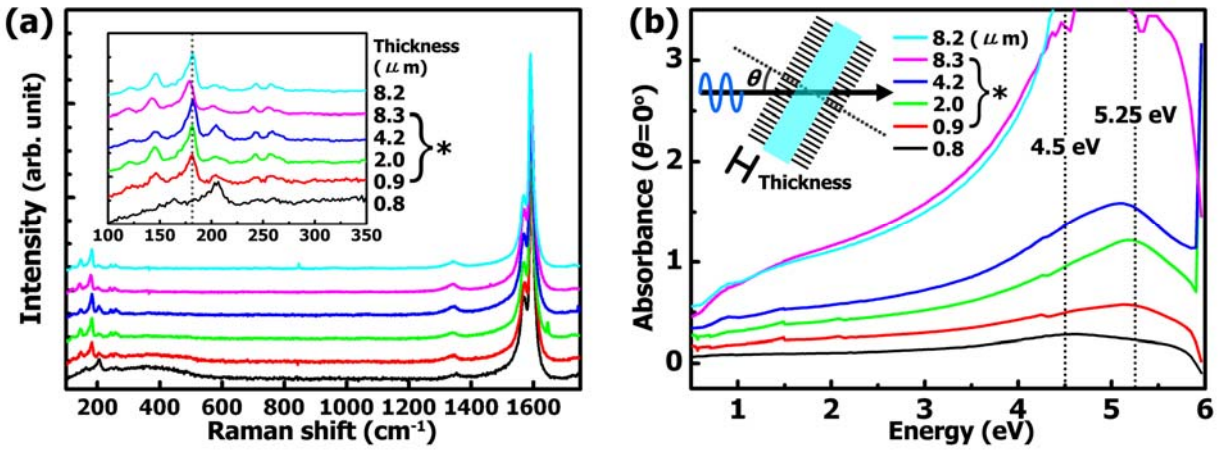

Fig. 3 − (a) Raman scattering and (b) optical absorption spectra of SWCNT films with specific thicknesses. (b) The absorption spectra measured with p-polarized incident light indicates that all the samples are actually in vertical alignment, except for the 0.8-μm-thick one. Samples marked with an asterisk meaning those made by the termination method.

We measured *I-V* curves of the VA-SWCNT films made by the termination method with electrodes on both sides. *I-V* curves of SWCNT films with different thicknesses, providing a good

fit to Ohm's law, are shown in Fig. 4a. The inset in Fig. 4a shows that the decrease of overall resistance during 100 sweeps is small (~ 2.4 %), promising the measurement stability. The reduction in resistance is attributed to that the defective SWCNTs burned away selectively at high current. The slopes here give resistances that are the sum of the film resistance, lead-wire resistance, and contact resistance, in series. The intrinsic resistance of SWCNT films could be obtained by eliminating the lead-wire resistance and contact resistance, as shown in Fig. 4b.

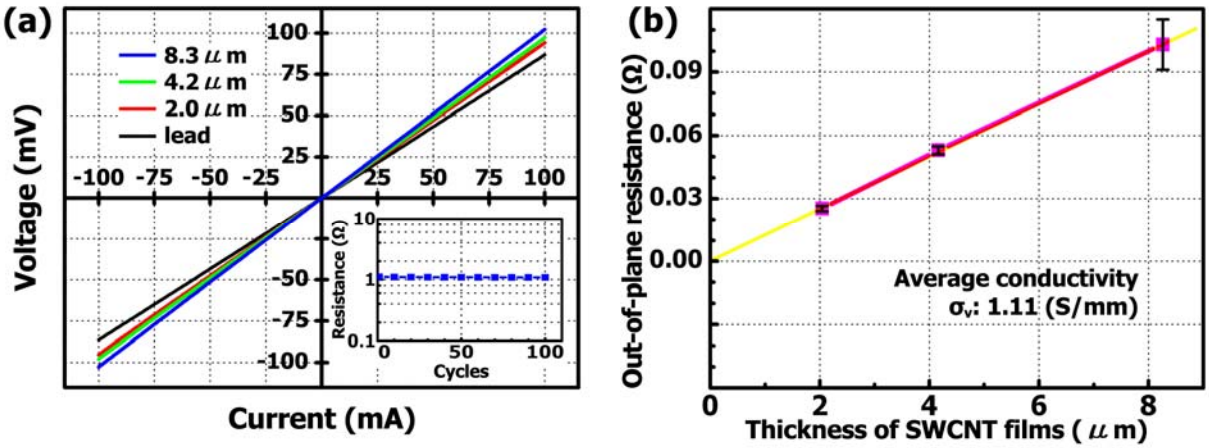

Fig. 4 − (a) Typical *I-V* characteristics of VA-SWCNT films measured along out-of-plane direction. The inset exhibits that the decay of the resistance measured during 100 sweeps is small. (b) Resistance versus sample thickness, indicating a linear fit. The intrinsic electrical properties were measured along out-of-plane direction of VA-SWCNT films.

To calculate the out-of-plane conductivity (σ_v) of SWCNT films, a general equation was used:

$$R_v = \left(\frac{1}{\sigma_v}\right)\left(\frac{t}{A}\right) \tag{1}$$

where R_v is the intrinsic out-of-plane resistance, σ_v is the conductivity perpendicular to the film

plane, t is the film thickness, and A is the effective conduction area. Here the effective conduction area was adopted instead of the contact area between electrodes, because in practice the SWCNTs only occupied a very small space in the bulk film. It is known that the mass density of SWCNT films is 0.036 g cm^{-3} [26], and the microscopic density of close-packed SWCNT bundles is assumed to be 2 g cm^{-3} [16]. The ratio of densities between them (1.8 %) is then utilized as the effective conduction area in our calculation. According to a good linear fit in Fig. 4b, the average conductivity was evaluated as 1.11 S/mm. This represents that the conductivity along the out-of-plane direction (σ_v) in the VA-SWCNT films is independent of film thickness. Similar measurement had been performed by Qu et al, but they didn't focus on studying the intrinsic electrical properties of SWCNT films [27]. The out-of-plane conductivity is close to that of close-packed SWCNT bundles (6.25 S/mm) [16], and that of vertically-aligned multi-walled CNT films (4 S/mm) [28].

The in-plane electron transport (sheet resistance) of VA-SWCNT films was studied by a four-probe measurement system. Sheet resistance in an infinite thin film is generally determined as,

$$R_s = \left(\frac{\pi}{\ln 2}\right)\left(\frac{V}{I}\right) = \frac{1}{\sigma_s t} \tag{2.1}$$

where R_s is sheet resistance, V/I term is the measured slope, σ_s is the conductivity along the in-plane direction of the film, and t is the film thickness. In our case, the size of SWCNT film relative to the spacing between probes is taken into account as a finite sample. Therefore two correction factors

have to be considered: shape factor (f_1) and thickness factor (f_2). According to the literature [29], f_1 and f_2 can be assigned to be 4.32 (at the ratio of sample width "12.5 mm" to probe spacing "1 mm": 12.5) and unity (as film thickness << probe spacing), respectively. It is emphasized that while the shape factor is used in calculation, the mechanism of electron hopping along the in-plane direction in our samples is different from that in thin-film materials. By using the modified equation:

$$R_s = 4.32\left(\frac{V}{I}\right) = \frac{1}{\sigma_s t} \tag{2.2}$$

the sheet resistance of VA-SWCNT films with different thicknesses was obtained and shown in Fig. 5a. The degradation of the resistance during 50 sweeps is negligible (Fig. S1). The results of electrical measurement are summarized in Table 1.

Table 1 − The anisotropic electrical properties of VA-SWCNT films.

Film thickness (μm)	Out-of-plane resistance (R_v, Ω)	Out-of-plane conductivity (σ_v, S/mm)	In-plane (sheet) resistance (R_s, kΩ/□)	In-plane (sheet) conductivity (σ_s, S/mm)
0.9	n/a[a]	n/a[a]	29.5	3.6×10^{-2}
2.0	0.025	1.13	19.7	2.5×10^{-2}
4.2	0.053	1.09	28.3	8.5×10^{-3}
8.3	0.103	1.11	25.5	4.8×10^{-3}

[a] The 1-μm-thick film is too thin thus it could not be peeled off from substrate without altering of the aligned morphology.

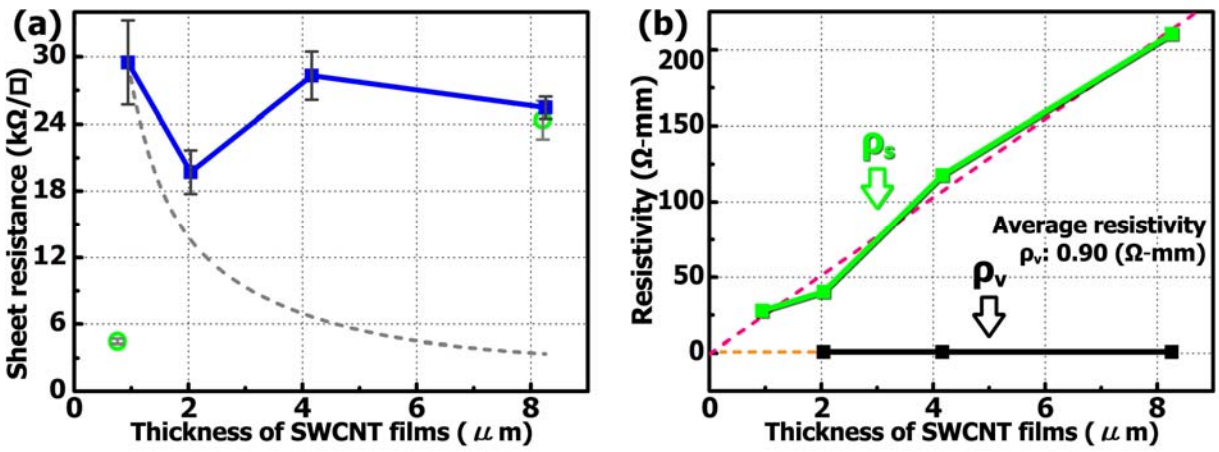

Fig. 5 − (a) In-plane resistances versus sample thicknesses. (b) Anisotropic electrical resistivities along out-of-plane (ρ_v) and in-plane (ρ_s) directions in VA-SWCNT films.

The average sheet resistance of VA-SWCNT films in Fig. 5a is ranging between 20 – 30 kΩ/□. It can be noticed that the result of the aligned sample obtained by saturation method (8.2 μm; green circle) is similar to that made by termination method (8.3 μm; blue square). On the other hand, the randomly-networked sample (0.8 μm; green circle) shows a much smaller sheet resistance (~ 15 %) than that of vertically-aligned one with similar thickness (0.9 μm). In a randomly-networked sample, the SWCNTs also grow horizontally and the electrons are transported along the nanotube axis rather than tunnel between nanotubes, resulting in the decrease of in-plane resistance. Therefore, we can conclude that the aligned morphology significantly affects the in-plane electrical conduction of VA-SWCNT films. The results also suggest that the synthesis method (termination or saturation) has minute influence on the electric conduction as long as the SWCNTs are aligned, despite the significant difference in growth rate and time in later stage of the growth.

While regarding the VA-SWCNT films as a continuous film structure, the in-plane

conductivity (σ_s) of samples can be calculated by equation (2.2). Table 1 shows the anisotropic electrical properties of the VA-SWCNT films. In-plane conductivity (σ_s) decreases with increasing film thickness, whereas the out-of-plane conductivity (σ_v) is independent of film thickness. The observation is abnormal because electron transport along a certain axis in bulk structure should exhibit size-independent conductivity at fixed temperature. For example, the conductivity in the basal plane of graphite crystals is ~ 2.6×10^5 S/mm and that perpendicular to the basal plane is in range of $(1.5 – 2.3) \times 10^3$ S/mm [30].

If the in-plane conductivity in the samples is constant with respect to the film thickness, the in-plane resistance should decay exponentially as the curve (gray dash line) in Fig. 5a, which is apparently not the case in the experimental results. The comparative plots in Fig. 5b show the out-of- and in-plane resistivities versus their film thickness. The resistivity is simply the reciprocal of conductivity. The linear fit of in-plane resistivities (ρ_s) implies that in VA-SWCNT system the in-plane resistance has approximately a constant value of 25.9 kΩ/□, and is independent of film thickness. Recently a morphological model was proposed, suggesting that a thin layer of randomly-oriented CNTs would be formed on top of VA-SWCNT film during the initial growth stage [31,32]. Such a model can expound the in-plane electrical behavior of our samples, in which the electron is principally hopping through the CNT networks on film surface, rather than across the junctions between VA-SWCNTs underneath it. The anisotropic conduction mechanism is schematically shown in Fig. 6. This model suggests that the vertically aligned part underneath the

surface layer has negligible contribution to the out-of-plane conductivity, which gives rise to a strong anisotropy, about hundred times stronger than that of previously reported SWCNT forests with different morphology [19].

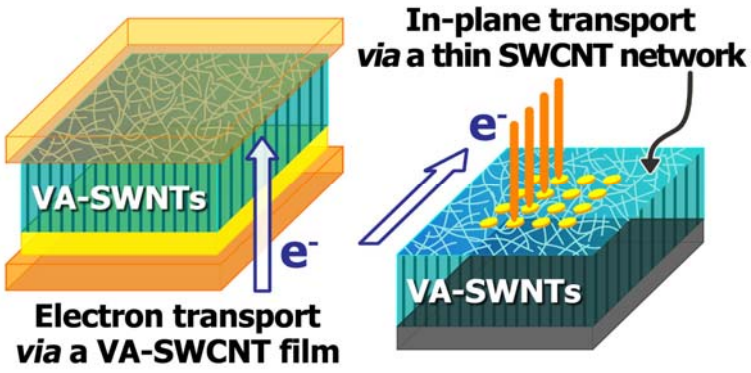

Fig. 6 − (Left) Electron conductance goes through the longitudinal axis of SWCNTs, resulting in an increased resistance with increasing of film thickness. (Right) Electron transports via a thin nanotube network which is unaffected by the thickness variation of VA-SWCNT films

4. Conclusions

The anisotropic conduction properties of VA-SWCNT films prepared under well-defined conditions have been determined by out-of- and in-plane measurements. The conductivity of VA-SWCNT films along out-of-plane direction (σ_v) is demonstrated to be about 1.11 S/mm and independent of film thickness. On the contrary, their in-plane (sheet) conductivity (σ_s) decreases with increasing film thickness, with the approximately thickness-independent sheet resistance (25.9 kΩ/□). The thickness-dependent in-plane conductivity can be explained by a growth model of vertically aligned SWCNT films, in which a thin layer of nanotube networks form on top of films at

the initial stage of the growth.

As a result, the in-plane conductivity was found to be more than an order of magnitude smaller, which gives rise to highly anisotropic electrical conduction, reflecting the high degree of alignment in the VA-SWCNT films. In addition, these properties were found be independent of the feedstock termination method as long as the SWCNTs are aligned. The above findings may be useful for application of SWCNTs in miniaturized sensing devices.

Acknowledgments. The authors would like to thank the National Science Council of the Republic of China, Taiwan, for financially supporting this research under contract number: NSC 96-2917-I-007-004.

References

[1] Pushparaj VL, Shaijumon MM, Kumar A, Murugesan S, Ci L, Vajtai R, et al. Flexible energy storage devices based on nanocomposite paper. Proc Natl Acad Sci U S A. 2007;104(34):13574-7.

[2] Jo SH, Tu Y, Huang ZP, Carnahan DL, Wang DZ, Ren ZF. Effect of length and spacing of vertically aligned carbon nanotubes on field emission properties. Appl Phys Lett. 2003;82(20):3520-2.

[3] Wang CY, Chen TH, Chang SC, Chin TS, Cheng SY. Flexible field emitter made of carbon nanotubes microwave welded onto polymer substrates. Appl Phys Lett. 2007;90(10):103111.

[4] Kang IP, Schulz MJ, Kim JH, Shanov V, Shi DL. A carbon nanotube strain sensor for structural health monitoring. Smart Mater Struct. 2006;15(3):737-48.

[5] Kong J, Franklin NR, Zhou CW, Chapline MG, Peng S, Cho KJ, et al. Nanotube molecular wires as chemical sensors. Science. 2000;287(5453):622-5.

[6] Huang CS, Huang BR, Jang YH, Tsai MS, Yeh CY. Three-terminal CNTs gas sensor for N-2 detection. Diam Relat Mater. 2005;14(11-12):1872-5.

[7] Collins PG, Bradley K, Ishigami M, Zettl A. Extreme oxygen sensitivity of electronic properties of carbon nanotubes. Science. 2000;287(5459):1801-4.

[8] Yu SG, Yi WK. Single-walled carbon nanotubes as a chemical sensor for SO2 detection. IEEE Trans Nanotechnol. 2007;6(5):545-8.

[9] Baker SE, Tse KY, Lee CS, Hamers RJ. Fabrication and characterization of vertically aligned

carbon nanofiber electrodes for biosensing applications. Diam Relat Mater. 2006;15(2-3):433-9.

[10] Alessandri I, Comini E, Bontempi E, Faglia G, Depero LE, Sberveglieri G. Cr-inserted TiO2 thin films for chemical gas sensors. Sens Actuator B-Chem. 2007;128(1):312-9.

[11] Murakami Y, Miyauchi Y, Chiashi S, Maruyama S. Direct synthesis of high-quality single-walled carbon nanotubes on silicon and quartz substrates. Chem Phys Lett. 2003;377(1-2):49-54.

[12] Maruyama S, Einarsson E, Murakami Y, Edamura T. Growth process of vertically aligned single-walled carbon nanotubes. Chem Phys Lett. 2005;403(4-6):320-3.

[13] Murakami Y, Maruyama S. Detachment of vertically aligned single-walled carbon nanotube films from substrates and their re-attachment to arbitrary surfaces. Chem Phys Lett. 2006;422(4-6):575-80.

[14] Dai HJ, Wong EW, Lieber CM. Probing electrical transport in nanomaterials: Conductivity of individual carbon nanotubes. Science. 1996;272(5261):523-6.

[15] Zhu LB, Xu JW, Xiu YH, Sun YY, Hess DW, Wong CP. Growth and electrical characterization of high-aspect-ratio carbon nanotube arrays. Carbon. 2006;44(2):253-8.

[16] Lee RS, Kim HJ, Fischer JE, Thess A, Smalley RE. Conductivity enhancement in single-walled carbon nanotube bundles doped with K and Br. Nature. 1997;388(6639):255-7.

[17] Fischer JE, Dai H, Thess A, Lee R, Hanjani NM, Dehaas DL, et al. Metallic resistivity in crystalline ropes of single-wall carbon nanotubes. Phys Rev B. 1997;55(8):R4921-R4.

[18] Pint CL, Xu YQ, Morosan E, Hauge RH. Alignment dependence of one-dimensional electronic hopping transport observed in films of highly aligned, ultralong single-walled carbon nanotubes. Appl Phys Lett. 2009;94(18):182107.

[19] Zhao B, Futaba DN, Yasuda S, Akoshima M, Yamada T, Hata K. Exploring Advantages of Diverse Carbon Nanotube Forests With Tailored Structures Synthesized by Supergrowth from Engineered Catalysts. Acs Nano. 2009;3(1):108-14.

[20] Futaba DN, Hata K, Yamada T, Hiraoka T, Hayamizu Y, Kakudate Y, et al. Shape-engineerable and highly densely packed single-walled carbon nanotubes and their application as super-capacitor electrodes. Nat Mater. 2006;5(12):987-94.

[21] Baumgartner G, Carrard M, Zuppiroli L, Bacsa W, deHeer WA, Forro L. Hall effect and magnetoresistance of carbon nanotube films. Phys Rev B. 1997;55(11):6704-7.

[22] Hone J, Llaguno MC, Nemes NM, Johnson AT, Fischer JE, Walters DA, et al. Electrical and thermal transport properties of magnetically aligned single wall carbon nanotube films. Appl Phys Lett. 2000;77(5):666-8.

[23] Kovtyukhova NI, Mallouk TE. Ultrathin anisotropic films assembled from individual single-walled carbon nanotubes and amine polymers. J Phys Chem B. 2005;109(7):2540-5.

[24] Zhang ZY, Einarsson E, Murakami Y, Miyauchi Y, Maruyama S. Polarization dependence of radial breathing mode peaks in resonant Raman spectra of vertically aligned single-walled carbon nanotubes. Phys Rev B. 2010;81(16):165442.

[25] Murakami Y, Einarsson E, Edamura T, Maruyama S. Polarization dependence of the optical

absorption of single-walled carbon nanotubes. Phys Rev Lett. 2005;94(8):087402.

[26] Xiang R, Yang Z, Zhang Q, Luo GH, Qian WZ, Wei F, et al. Growth deceleration of vertically aligned carbon nanotube arrays: Catalyst deactivation or feedstock diffusion controlled? J Phys Chem C. 2008;112(13):4892-6.

[27] Qu L, Dai L. Gecko-foot-mimetic aligned single-walled carbon nanotube dry adhesives with unique electrical and thermal properties. Adv Mater. 2007;19(22):3844-9.

[28] Li XS, Ci L, Kar S, Soldano C, Kilpatrick SJ, Ajayan PM. Densified aligned carbon nanotube films via vapor phase infiltration of carbon. Carbon. 2007;45(4):847-51.

[29] Smits FM. Measurement of sheet resistivities with the four-point probe. Bell Labs Tech J. 1958;37:711-8.

[30] Primak W, Fuchs LH. Electrical conductivities of natural graphite crystals. Phys Rev. 1954;95(1):22-30.

[31] Zhang L, Li ZR, Tan YQ, Lolli G, Sakulchaicharoen N, Requejo FG, et al. Influence of a top crust of entangled nanotubes on the structure of vertically aligned forests of single-walled carbon nanotubes. Chem Mater. 2006;18(23):5624-9.

[32] Zhang Q, Zhou WP, Qian WZ, Xiang R, Huang JQ, Wang DZ, et al. Synchronous growth of vertically aligned carbon nanotubes with pristine stress in the heterogeneous catalysis process. J Phys Chem C. 2007;111(40):14638-43.

Supplemental Materials

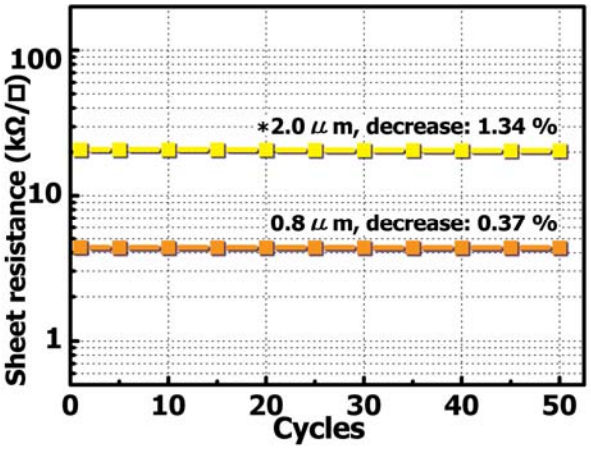

Fig. S1 − Sheet resistances of VA-SWCNT films measured for repetitive sweeps over 50 times using a four-probe method. A trace of the decrease of sheet resistances manifests that the measurements are reproducible and do not change the sample properties. Samples marked with an asterisk meaning those made by the termination method.

Figure 1

Click here to download high resolution image

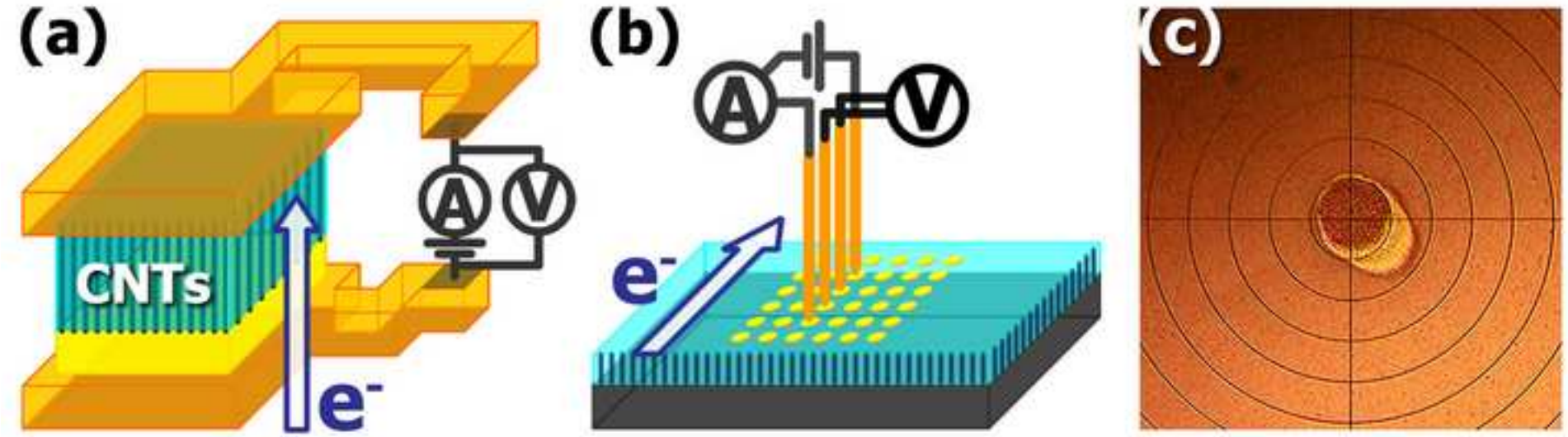

Figure 2a

Click here to download high resolution image

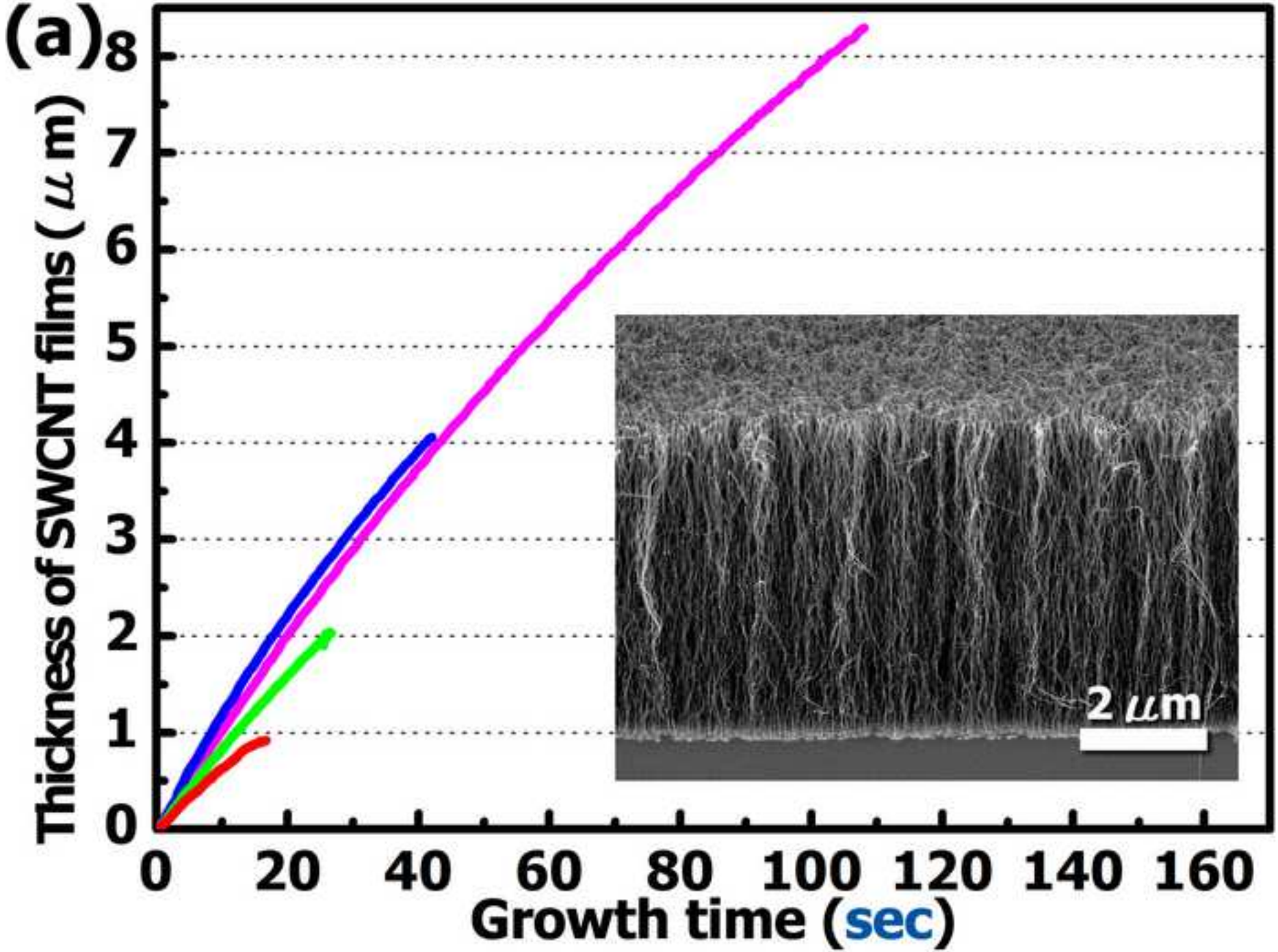

Figure 2b

Click here to download high resolution image

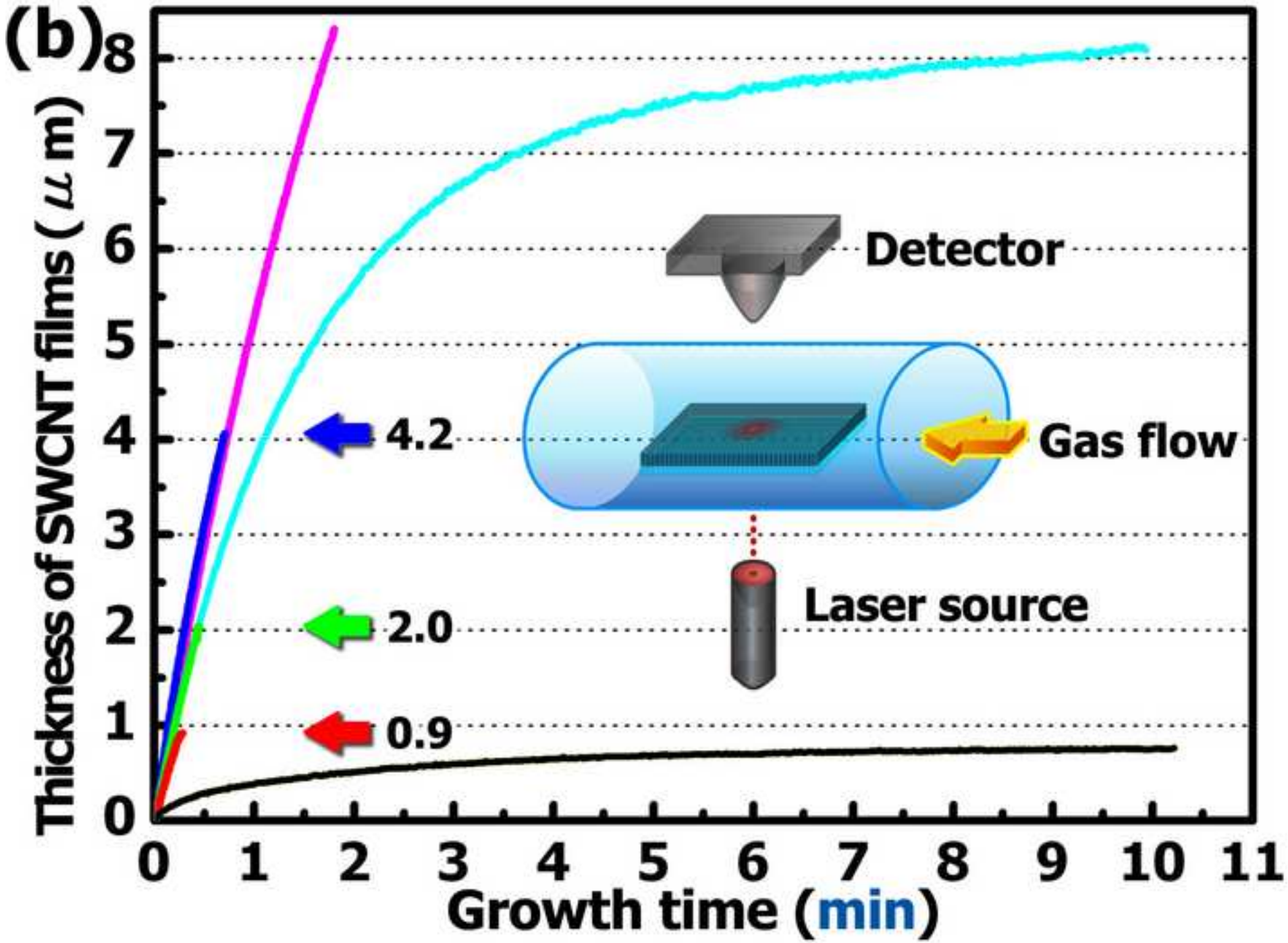

Figure 3a

Click here to download high resolution image

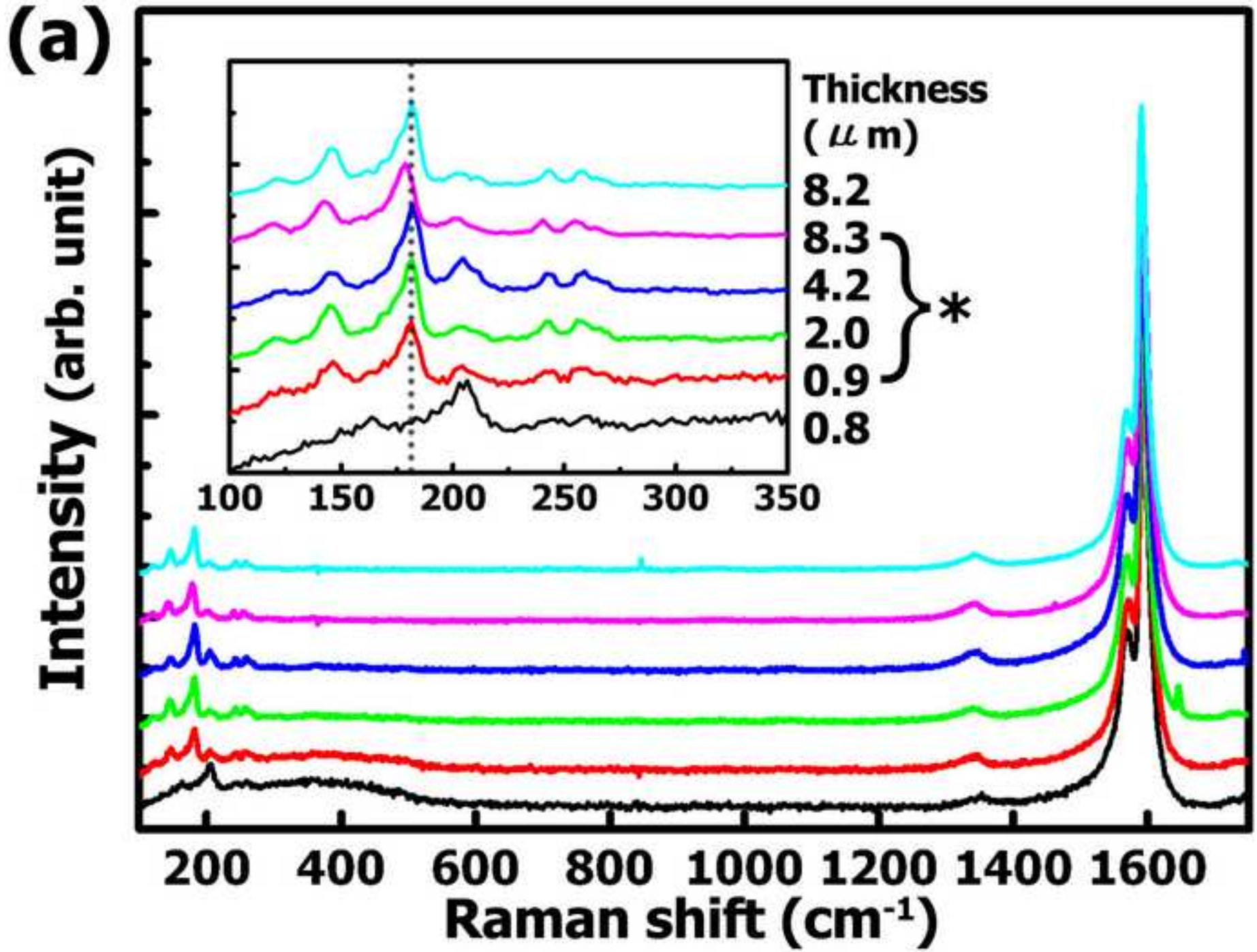

Figure 3b

Click here to download high resolution image

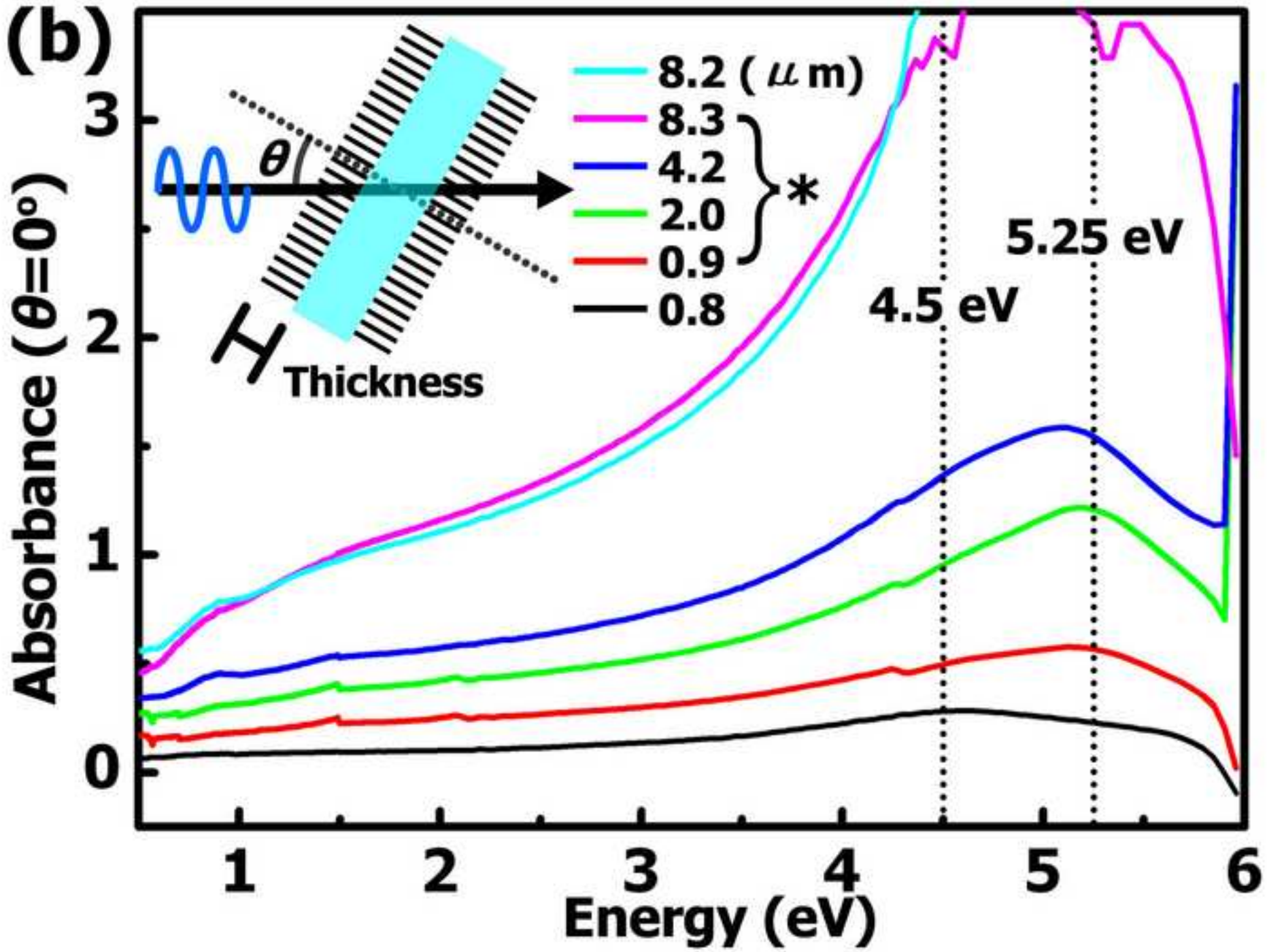

Figure 4a

Click here to download high resolution image

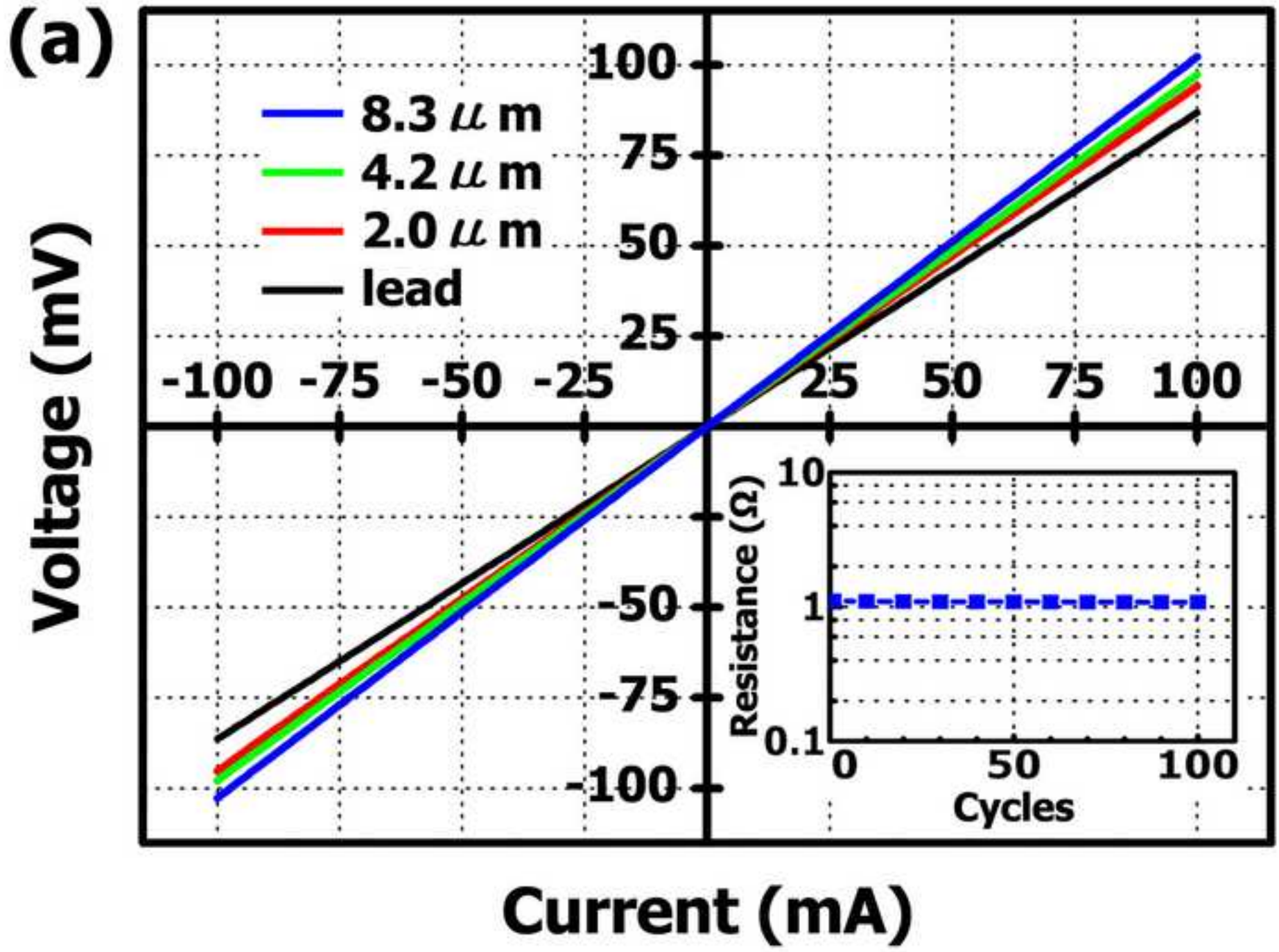

Figure 4b

Click here to download high resolution image

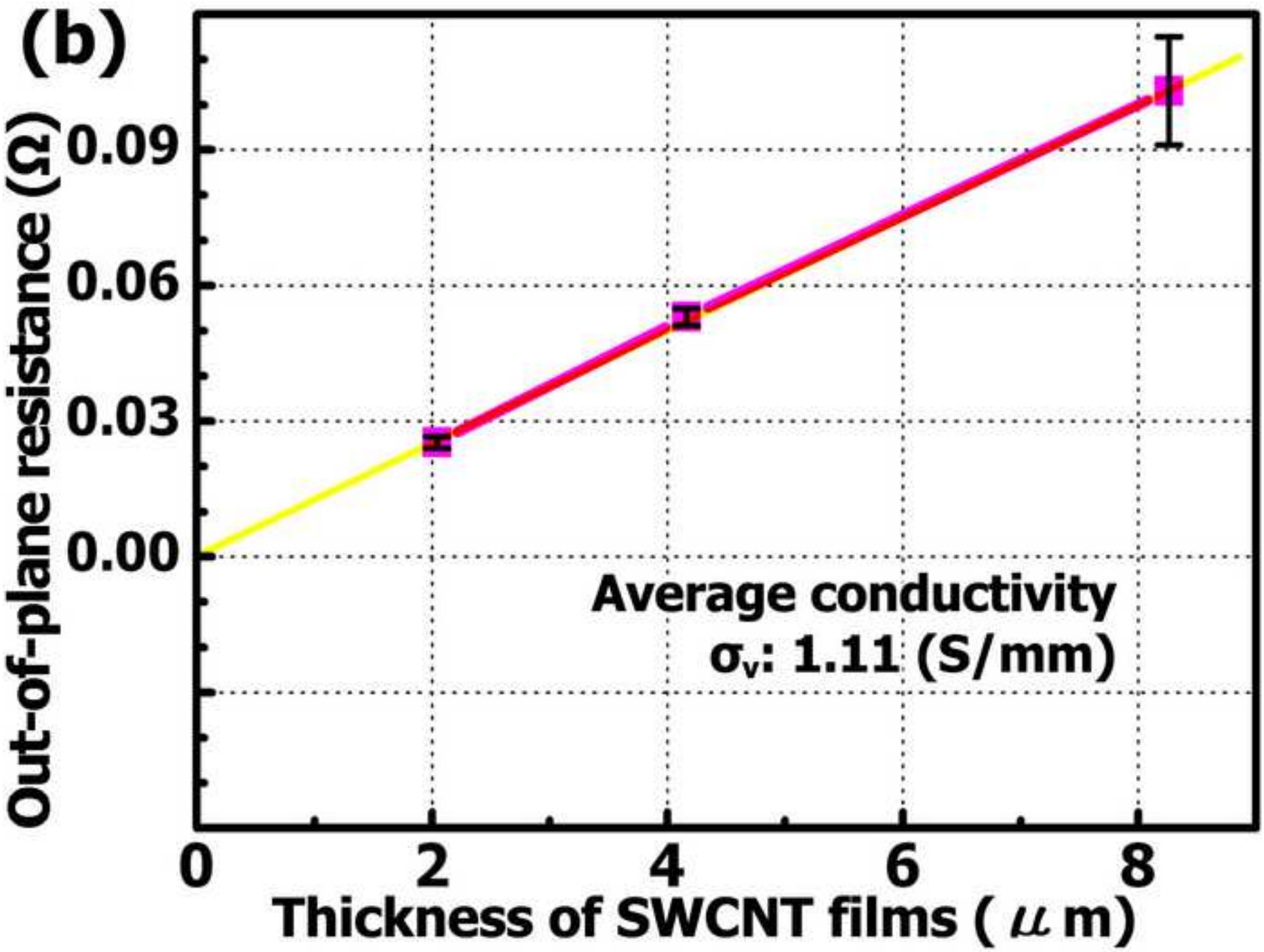

Figure 5a

Click here to download high resolution image

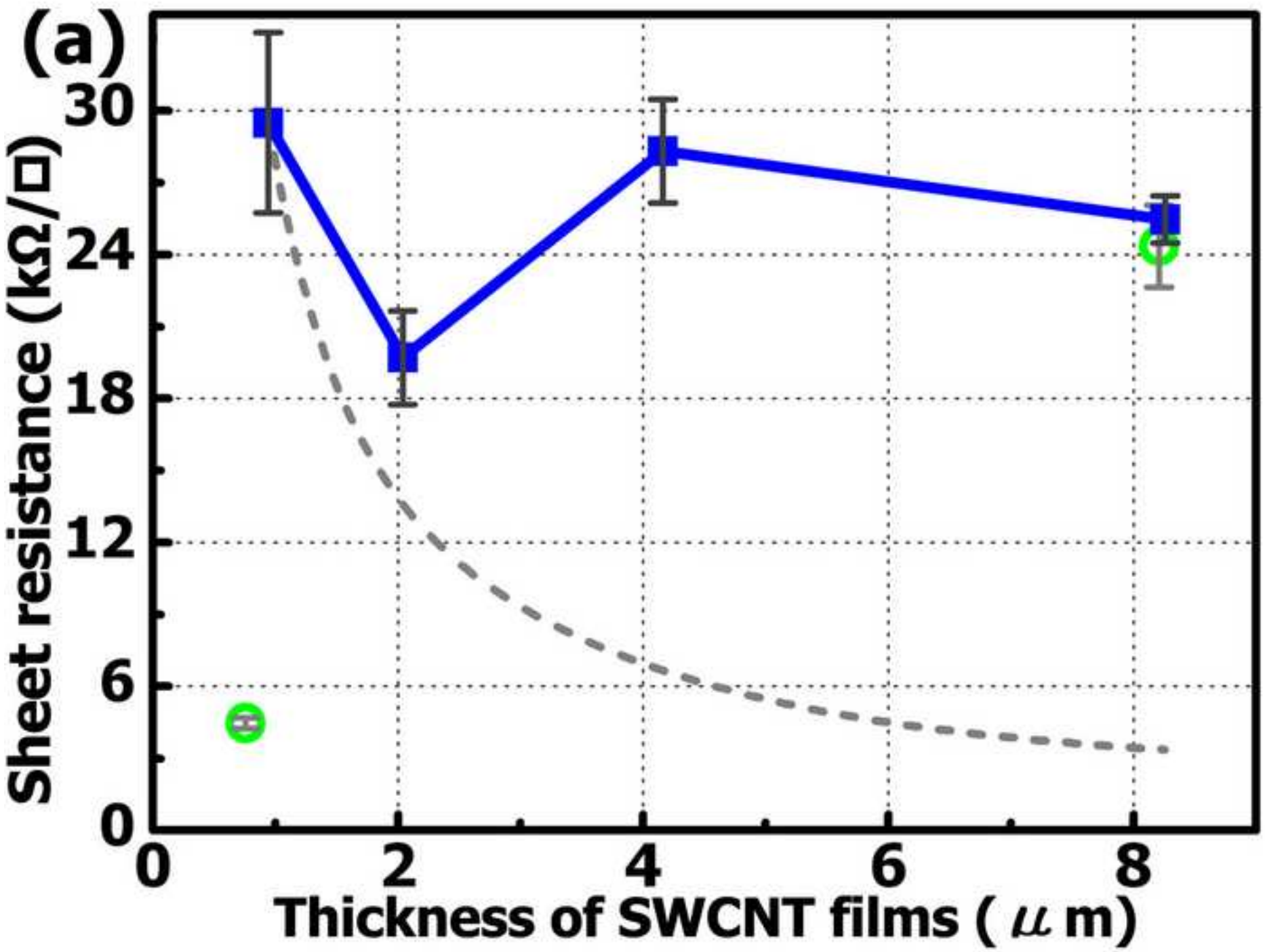

Figure 5b

Click here to download high resolution image

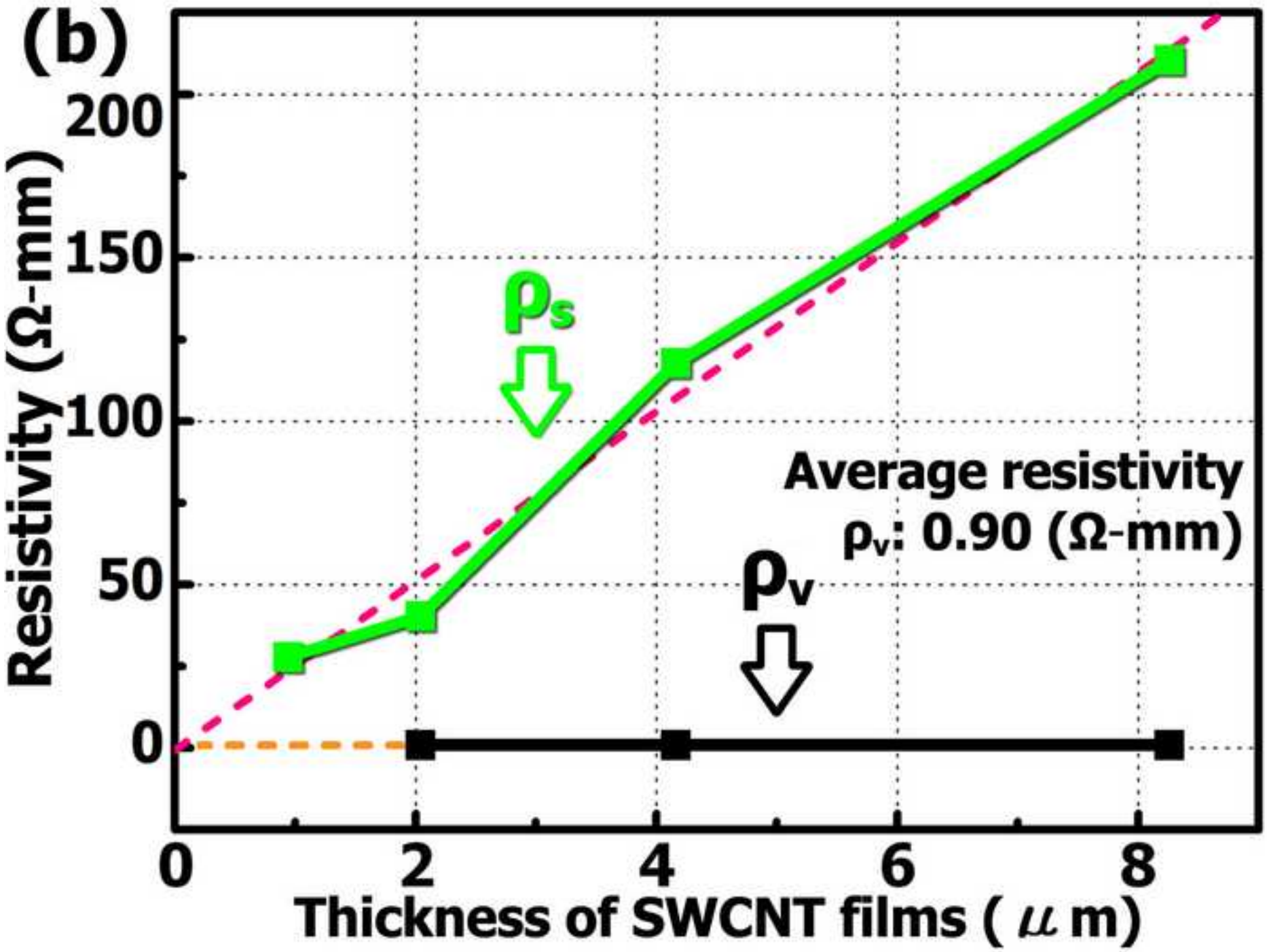

Figure 6
Click here to download high resolution image

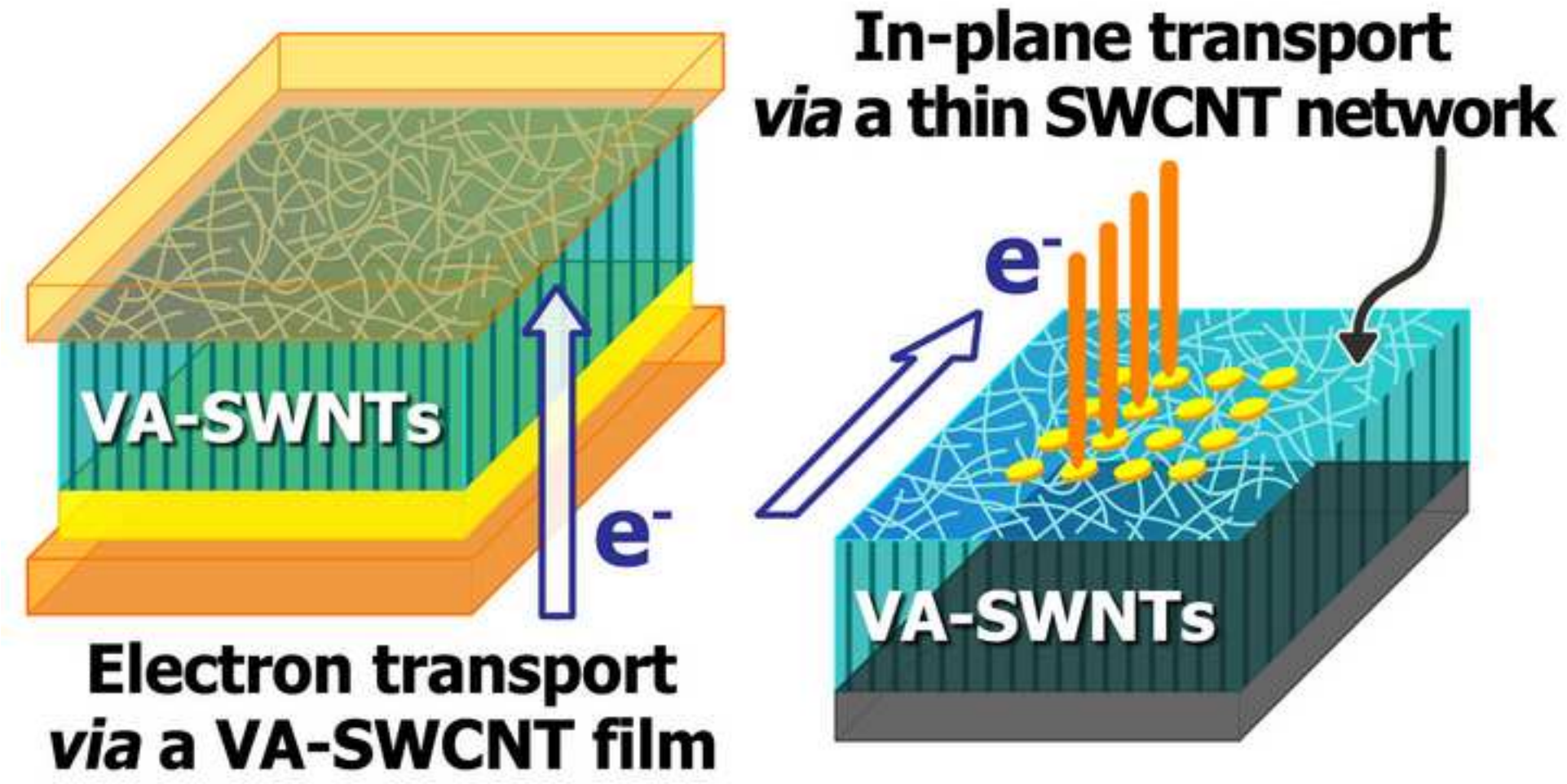

Figure S1

Click here to download high resolution image